

## Original Article

**Cite this article:** Pandey DK, Pandey A, Clift PD, Nair N, Ramesh P, Kulhanek DK and Yadav R (2020) Flexural subsidence analysis of the Laxmi Basin, Arabian Sea and its tectonic implications. *Geological Magazine* 157: 834–847. <https://doi.org/10.1017/S0016756818000833>

Received: 30 April 2018

Revised: 29 October 2018

Accepted: 29 October 2018

First published online: 18 December 2018




**Keywords:**

continental rifting; flexural subsidence; Laxmi Basin; Site U1457; IODP Expedition 355; Arabian Sea; JOIDES Resolution

**Author for correspondence:**

D. K. Pandey, Email: [pandey@ncaor.gov.in](mailto:pandey@ncaor.gov.in)

# Flexural subsidence analysis of the Laxmi Basin, Arabian Sea and its tectonic implications

D. K. Pandey<sup>1</sup> , Anju Pandey<sup>1</sup>, Peter D. Clift<sup>2</sup>, Nisha Nair<sup>1</sup> , Prerna Ramesh<sup>1</sup>, Denise K. Kulhanek<sup>3</sup>  and Rajeev Yadav<sup>1</sup>

<sup>1</sup>ESSO–National Centre for Polar and Ocean Research, Goa 403804, India; <sup>2</sup>Department of Geology and Geophysics, Louisiana State University, Baton Rouge, Louisiana 70803, USA and <sup>3</sup>International Ocean Discovery Program, Texas A&M University, College Station, Texas 77845, USA

**Abstract**

Two-dimensional flexural backstripping and thermal modelling (assuming laterally variable stretching) is applied along regional depth-converted interpreted seismic profiles from the Laxmi Basin in the Arabian Sea. Results from reverse post-rift flexural modelling reveal considerable basin-wide subsidence in response to the crustal geodynamics during and after the last extensional phase. Unloading of the stratigraphy allows us to estimate the degree of laterally varying extension, assuming thermal subsidence and pure shear. High degrees of extension in the basin centre predict considerable water depths at the time of rift cessation, consistent with deep drilling data. We suggest that regional extension prior to Paleocene time could have fuelled variable subsidence in the Laxmi Basin but that extension is less than seen in typical oceanic lithosphere. Volcanic loading by the seamounts shortly after extension has flexed the basin and implies an effective elastic thickness ( $T_e$ ) at that time of  $\sim 6$  km. Reconstruction of the seamount top near sea level at the end of emplacement indicates no major transient uplift potentially linked to the Deccan mantle plume activity. Backstripping of post-rift sediments from interpreted seismic profiles supports the presence of a hyper-thinned crust underneath the Laxmi Basin, with  $\beta$  factors reaching  $>7$  in the basin centre and  $\sim 3$  across much of the basin width. Computations of decompacted sediment accumulation rates in light of new results from IODP Expedition 355 show that basin sedimentation peaked during early–middle Miocene time, possibly coeval with uplift and erosion of the Himalayan–Tibetan Plateau driven by strong summer monsoon rains.

**1. Introduction**

Rifted continental margins preserve unique records of thermo-tectonic evolution that can be deduced from the history of basement subsidence (McKenzie, 1978; White & McKenzie, 1989; Allen & Allen, 2006). Passive margins also hold the key to unravelling the processes operating during rift to drift transition depending upon whether or not new oceanic crust was generated. Therefore, rift margins proximal to relatively young ocean basins may provide crucial information concerning the prevailing crustal architecture, as well as the nature of strain accommodation (McKenzie & Sclater, 1971; Kuszniir *et al.* 1995; Watts, 2001). Thermo-mechanical processes during early basin evolution (i.e. active extension) ultimately translate into various forms of lateral and vertical tectonics causing subsequent margin uplift/subsidence/shearing (Royden & Keen, 1980). Considerable subsidence at rifted passive margins and adjoining areas has been reported for several decades, reflecting high degrees of extension in these settings (Baxter *et al.* 1999; Allen & Allen, 2006). Therefore, determining long-term total subsidence (tectonic as well as thermal) along passive margins allows a precise extensional history to be reconstructed (Watts, 2001; Allen & Allen, 2006). Post-rift sediment thicknesses developed beneath the outer shelf and slope range from a few hundreds of metres to a few kilometres in the Arabian Sea (Kolla & Coumes, 1987; Clift *et al.* 2002). However, some of the thickest passive margins, such as the western continental margin of India (WCMI), still remain under-explored in terms of margin subsidence analysis (Whiting *et al.* 1994). This is primarily owing to the lack of deep-penetrating, high-quality regional seismic data, as well as lithological constraint from boreholes. Here we combine interpretation of high-quality seismic data with results from scientific drilling in the Laxmi Basin adjoining the WCMI to examine the nature of basin formation and subsequent evolution. Numerous earlier studies have been carried out using 1-D backstripping analyses close to the western Indian shelf edge in order to reconstruct the geological history from the basin stratigraphy (e.g. Mohan, 1985; Agrawal & Rogers, 1992; Whiting *et al.* 1994; Chand & Subrahmanyam, 2003; Calvès *et al.* 2008). However, these investigations primarily relied upon scattered observations and 1-D Airy type isostatic compensation (Watts, 2001). Airy type (i.e. local) isostasy has potential limitations because it does not account for the flexural strength of the lithosphere. Consequently, it tends to work well with a low effective elastic thickness (i.e.  $T_e \approx 0$ ) and overestimates stretching factors (Kuszniir *et al.* 1995;

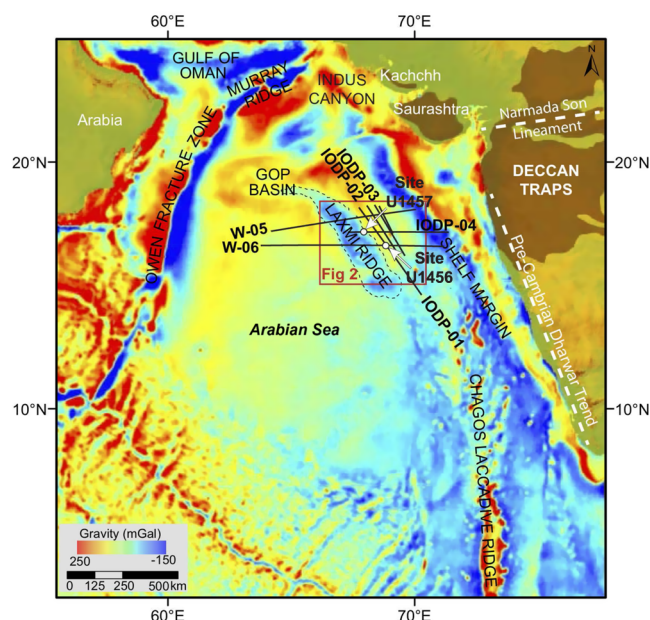


**Fig. 1.** Map of the study area with shaded topography shown onshore and a satellite-derived free air gravity anomaly map offshore. Alternating coast-parallel highs and lows correspond to various isolated tectonic elements, basement reliefs and horst and graben patterns. Solid black lines indicate the location of the new multi-channel seismic profiles across the Laxmi Basin. Two drill sites from IODP Expedition 355 are plotted on the map.

Roberts *et al.* 1998). The flexural approach accounts for lateral loads and produces more reliable subsidence estimates. The primary objective of this study is to investigate total subsidence in the Laxmi Basin using a 2-D flexural backstripping process.

## 2. Regional tectonic framework

Located in the eastern Arabian Sea, the WCMI is a passive continental margin that extends more than 2000 km from the Gujarat coast in the north to the Kerala coast in the south (Fig. 1). Major tectonic events in the past that shaped this margin include: (1) break-up of Greater India (India–Madagascar) from Africa *c.* 130–120 Ma; (2) the India–Madagascar break-up *c.* 88 Ma; (3) opening of the Gop Rift and Laxmi Basin in latest Cretaceous time; and (4) separation of the Seychelles from India (McKenzie & Sclater, 1971; Whitmarsh, 1974; Naini & Talwani, 1982; Storey *et al.* 1995; Biswas, 1999; Chaubey *et al.* 2002; Minshull *et al.* 2008; Gaina *et al.* 2015). The emplacement of the Deccan flood basalts at *c.* 65 Ma is believed to be simultaneous with the Seychelles–India rifting (Courtillot *et al.* 1986; Venkatesan *et al.* 1993; Collier *et al.* 2008). The poly-phase rifting finally culminated in seafloor spreading in the Arabian Sea and formation of the western Indian passive margin (Miles *et al.* 1998; Royer *et al.* 2002).

The shelf break along the WCMI occurs at an average water depth of ~200 m. However, water depths in the deeper basin range between ~3000 and 3600 m (Fig. 2). The shelf width along the WCMI varies greatly from north to south (Fig. 1). NW–SE-trending normal-faulted horst and graben structures separated by orthogonal cross faults have been reported by previous studies from the shelf margin. These deformations gave rise to several isolated tectonic blocks and marginal highs (Biswas, 1982, 1989; Mitra *et al.* 1983; Rao & Srivastava, 1984; Mohan, 1985; Whiting *et al.* 1994; Gombos *et al.* 1995; Nair *et al.* in review). Several large-scale

structural blocks of anomalous character (e.g. the Laxmi Ridge, Panikkar Ridge, Laxmi Basin) are identified along the margin, and these are located between the shelf edge and the deeper basins (Fig. 1). The enigmatic geophysical signatures of these anomalous features inhibit their precise fit within a reconstructed Gondwana. The Laxmi Ridge is generally regarded as a continental sliver (Naini & Talwani, 1982; Krishna *et al.* 2006) separated from the WCMI by the Laxmi Basin (Fig. 2). In contrast, the Laxmi Basin is variously proposed to comprise either oceanic crust including an extinct spreading centre or highly thinned continental crust. A NW–SE-trending series of isolated highs east of the Laxmi Ridge (e.g. the Wadia Guyot, Panikkar and Raman seamounts) are collectively referred to as the Panikkar Ridge. The oldest undisputed marine magnetic anomalies reported from this region are anomalies 27n (62.2–62.5 Ma) and 28n (63.5–64.7 Ma), located southwest of the Laxmi Ridge in the Arabian Basin and north of the Seychelles, respectively (Miles *et al.* 1998; Chaubey *et al.* 2002; Royer *et al.* 2002) (Fig. 2). Considerably older anomalies within the Laxmi Basin are also reported (Bhattacharya *et al.* 1994; Eagles & Wibisono, 2013; Bhattacharya & Yatheesh, 2015); however, their interpretation is controversial because of their short segments and uncertainties in correlation with geomagnetic time scales. Some researchers opine that, instead, these anomalies could be explained through the presence of dykes intruded within hyper-extended continental crust (e.g. Naini & Talwani, 1982; Krishna *et al.* 2006). While the longstanding debate about its precise crustal affinity continues, the role of vertical tectonics in this region has seldom been elucidated. A precise crustal affinity of the Laxmi Basin could be ascertained from the basaltic igneous basement sampled in the Laxmi Basin during International Ocean Discovery Program (IODP) Expedition 355 (Pandey *et al.* 2016). However, here we focus on the role of vertical tectonics as a flexural response to the thermo-tectonic developments in the Laxmi Basin.

## 3. Data and methodology

The 2-D post-rift subsidence analysis discussed here is based on subsurface information derived from representative seismic reflection profiles in the Arabian Sea. A grid of 5000 km of new 2-D multi-channel seismic (MCS) reflection data was acquired by the National Centre for Polar and Ocean Research (NCPOR) using a 6 km long streamer and 50 m shot spacing. We used three E–W (dip lines) and three NW–SE (strike lines) profiles (IODP-01, IODP-02, IODP-03, IODP-04, W-05 and W-06) of variable lengths (220–470 km; Fig. 2). The seismic profiles are long enough to capture basin-wide structural and sedimentation patterns. Stratigraphic interpretations of these seismic profiles are discussed in Nair *et al.* (in review). A high-resolution multi-beam bathymetry map (Fig. 2) shows the various morpho-tectonic features around the Laxmi Basin. Post-stack, time-migrated seismic sections were depth converted using interval velocities estimated from stacking velocities (Nair *et al.* in review). A representative depth-converted cross-section with seismic velocities superposed on it is presented in Figure 3. The interval velocities used for the time-depth conversion are in good agreement with those reported in published seismic refraction studies (Naini & Talwani, 1982; Minshull *et al.* 2008). Additional constraints are obtained from available lithological ground-truthing by dredging, coring (Kolla & Coumes, 1987; Mohanty *et al.* 2013; Misra *et al.* 2015; Pandey *et al.* 2017) and deep boreholes (Mohan, 1985; Whiting *et al.* 1994; Pandey *et al.* 2016). Considering the high data quality and constrained velocity analyses, uncertainties in time-depth conversion are estimated to be within

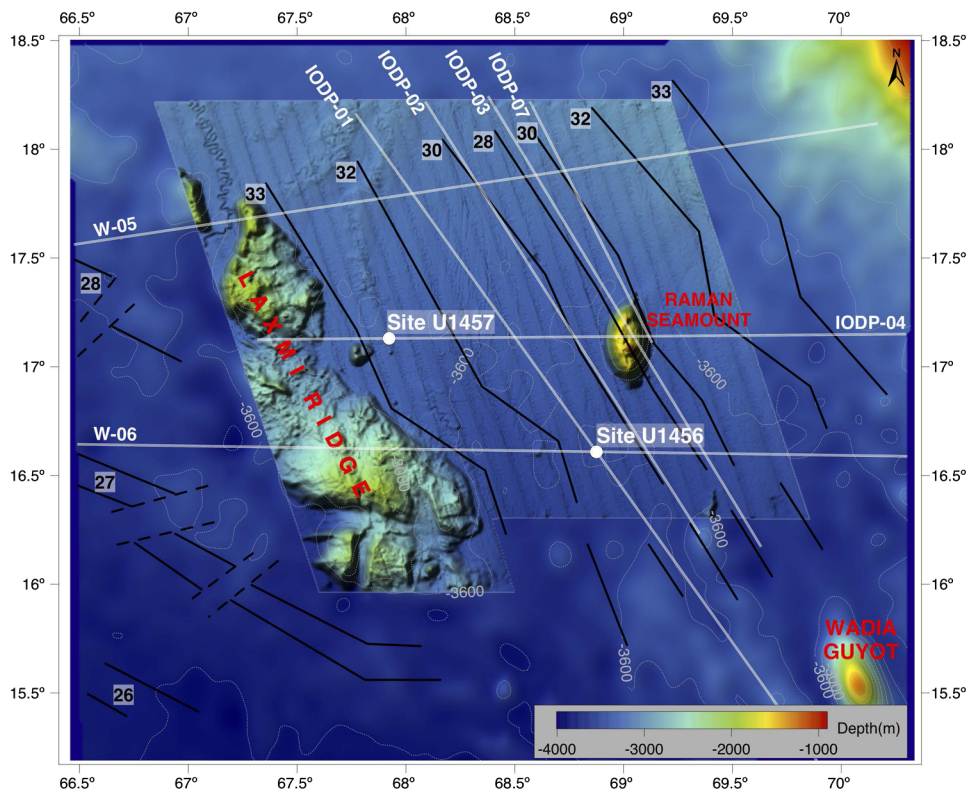


**Fig. 2.** Composite high-resolution multi-beam bathymetric map of the Laxmi Basin. Superposed are major tectonic elements and locations of the seismic profiles used in this study. Locations of IODP Sites U1456 and U1457 in the eastern Arabian Sea are shown (Pandey *et al.* 2016). Magnetic anomalies are plotted after Bhattacharya *et al.* (1994) and Bhattacharya & Yatheesh (2015).

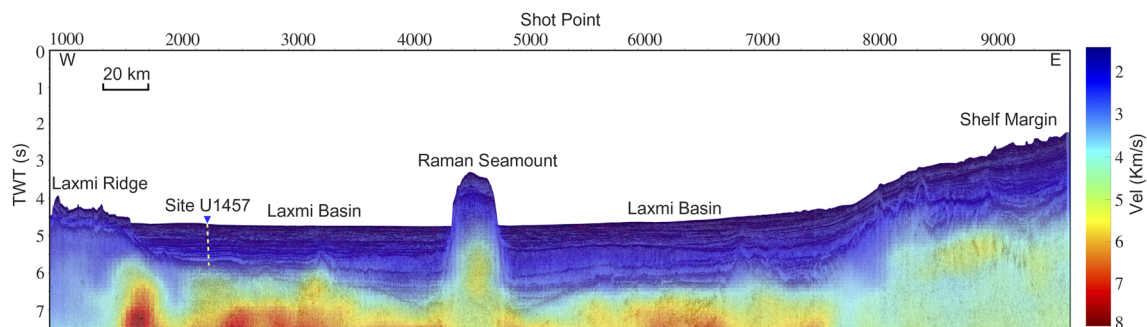


**Fig. 3.** A representative post-stacked, time-migrated seismic section along the dip profile IODP-04. An interval velocity grid obtained from stacking velocities is superimposed on the image to emphasize good coherency for the velocity-depth model. Different crustal domains are marked on the section. This velocity grid was used for the time-depth conversion. Note the location of IODP Site U1457 on this profile. The total depth (TD) at Site U1457 was 1109 m below seafloor where igneous basement was recovered under ~1090 m of Cenozoic sediment cover (see Pandey *et al.* 2016 for more details). TWT – two-way travel time.

10 %. Various seismic horizons and other structural elements were marked and picked using the Kingdom<sup>TM</sup> software. The overall stratigraphic framework in the Arabian Sea has been periodically modified by influx of sediments from the Indus Fan, as well as from the WCMI (Kolla & Coumes, 1987; Clift & Gaedicke, 2002). Four major stratigraphic units spanning the Paleocene–Recent and overlying igneous basement are identified (Table 1). Major unconformities dating back to early–middle Miocene time were constrained by lithological and biostratigraphic information from IODP sites U1456 and U1457 (Pandey *et al.* 2016), while deeper buried units, especially on the shelf, were constrained using industrial boreholes (Mohan, 1985; Whiting *et al.* 1994). A regional satellite-derived free air gravity anomaly map of the Laxmi Basin is shown in Figure 1. An E–W alternating high and low gravity anomaly pattern corresponds

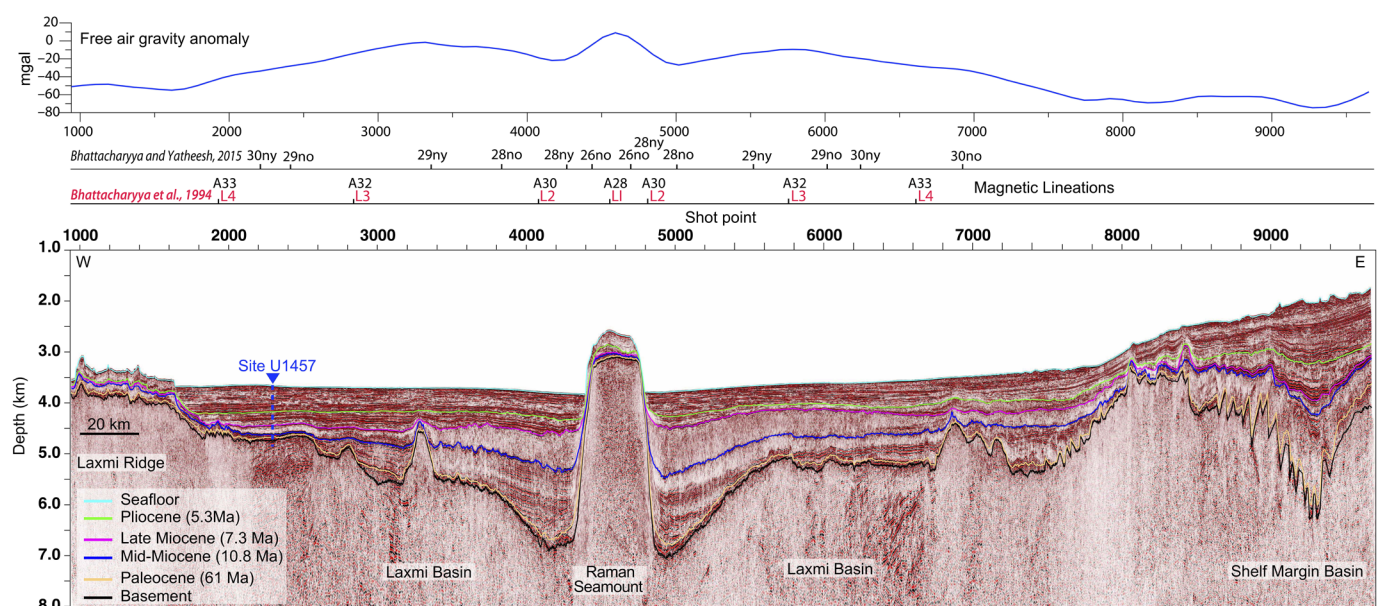
to the coast-parallel ridges and adjoining depressions (Biswas, 1982). The elevated seamounts in the Laxmi Basin exhibit a distinct high gravity anomaly embedded within a broad regional low (Fig. 1). The shelf edge is marked by relatively high free air gravity anomalies with amplitudes reducing seawards.

#### 4. Flexural reverse post-rift modelling

We have adopted a flexural backstripping approach to examine vertical tectonics and estimate extension (Kuszniir *et al.* 1995, 2004; Roberts *et al.* 1998). We used the FlexDecomp<sup>TM</sup> software package to determine variations in temporal and spatial subsidence around the Laxmi Basin. MCS data reveal variable sediment cover (Paleocene to Recent) overlying an igneous basement (Fig. 4).

**Table 1.** Various physical parameters used for the flexural modelling. See text for more details

Horizon at the base of stratigraphic unit	Age of the base of lithological unit (Ma)	Initial porosity (%)	Compaction constant ( $\text{km}^{-1}$ )	Velocity (km/s)	Matrix density ( $\text{gm cm}^{-3}$ )
Seabed	0	–	–	–	–
Pliocene–Recent	5.33	61	0.44	1.6	2.68
Upper Miocene	7.3	56	0.45	2.0	2.69
Mid Miocene	10.9	57	0.44	2.2	2.67
Paleocene	61.0	55	0.45	3.8	2.74
Top of Raman Seamount	65.5	0	0	4.5	2.8
Top basement	66.0	–	–	4.5	–
General modelling parameters					
Upper crust	–	–	–	6.3–6.5	2.7
Lower crust	–	–	–	7.1–7.2	3.0
Mantle	–	–	–	7.9–8.0	3.3

**Fig. 4.** (a) A depth-converted seismic section with various interpreted horizons overlain. Different sedimentary sequences are constrained using lithological information obtained from IODP Site U1457. The top panel represents free air gravity anomaly variations across the entire length of the seismic profile. Locations of short magnetic lineations (L1–L4) reported by Bhattacharya *et al.* (1994) and Bhattacharya & Yatheesh (2015) are marked above the reflection seismic image.

From bottom to top, these correspond to the Paleocene, middle Miocene, late Miocene and Pliocene–Recent, respectively. The deepest sedimentary horizon is interpreted as Paleocene (~61 Ma) based on recovery of a biostratigraphic assemblage of lower Paleocene forms at Site U1457 (Pandey *et al.* 2016). Numerical ages were estimated using the shipboard biostratigraphy (Fig. 6) following the revised Geological Time Scale of Gradstein *et al.* (2012). Using interpreted seismo-geologic cross-sections from the Laxmi Basin, the multi-step restoration process is achieved by removing the topmost (youngest) stratigraphic unit and allowing decompaction of the underlying units (Sclater & Christie, 1980). Decompaction is dependent on the lithology of the sequences, and for our purposes we use the drilling data from the IODP wells,

with an intermediate silt size used when this is in doubt. In performing the unloading procedure we also included the Raman and Panikkar seamounts as part of this procedure as they clearly post-date the initial extension in the basin, although the regional geology and seismic constraints indicate that they were emplaced shortly after the end of extension, so we assign an age of emplacement of slightly after 66 Ma, i.e. 65.5 Ma.

Further, incremental post-rift total subsidence corresponding to the ages of the removed stratigraphic units is computed using a variable stretching factor ( $\beta$ ) and the rift age, which we here estimate to be 66 Ma (latest Cretaceous). Next, the flexural isostatic response due to the removed mass of sediment matrix and water, as well as thermal subsidence, is determined. This process is

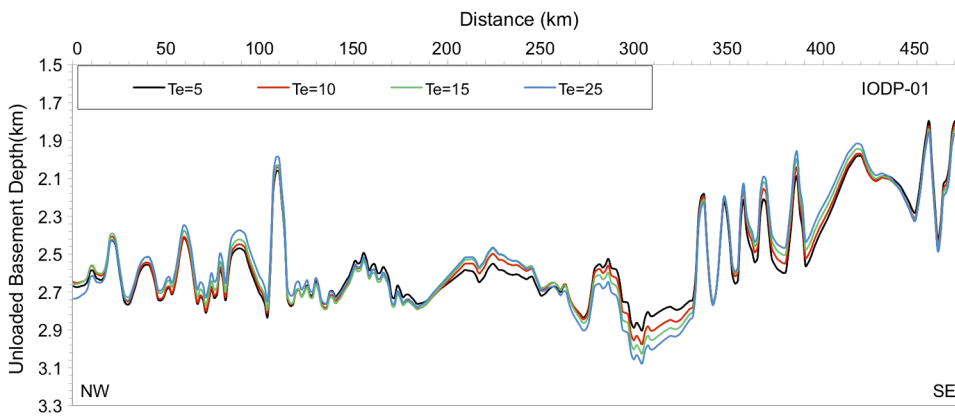


**Fig. 5.** Sensitivity analyses for showing the predicted unloaded depth to basement at the present day for different flexural strengths ( $T_e$ ). A  $T_e$  value of 6 km is preferred for the present study, especially keeping in view the width of the flexural moat around the Raman Seamount.

repeated sequentially until all post-rift stratigraphic units have been removed. The section resulting from unloading the basement in the above manner provides knowledge about the basement topography that would be present today had there been no sediment deposition since its formation. Assuming uniform extension, unloaded depths to basement can be used to estimate the degree of extension ( $\beta$  factor, defined as the ratio of the pre-rift lithosphere compared to the post-rift).

Although the precise onset of crustal extension in the Laxmi Basin is debated, the magnetic lineations in the Laxmi and Gop basins (Figs 2, 4) point towards active rifting in Late Cretaceous to possibly early Paleocene times (Biswas, 1982; Bhattacharya & Yatheesh, 2015). An older extensional event involving the Laxmi Basin and adjoining regions is also contemplated in view of the India–Madagascar break-up (Storey *et al.* 1995). However, its exact extent could not be ascertained because of the lack of deeper stratigraphic constraints. Palaeogeographic reconstruction models suggest that the latest rift phase in the Laxmi Basin initiated at ~75 Ma and ceased during late Paleocene time (c. 64 Ma) (Eagles & Wibisono, 2013; Bhattacharya & Yatheesh, 2015 and references therein). This is short enough to allow us to use the assumption of instantaneous stretching that is implied by the simplest uniform pure shear extensional models (Jarvis & McKenzie, 1980).

Flexural backstripping modelling is sensitive to the palaeo-bathymetry and past sea level undulations, especially close to the shelf edge (Allen & Allen, 2006). Palaeo-bathymetry interpretations from Mohan (1985), Zutshi *et al.* (1993), Nair *et al.* (1992) and Mathur & Nair (1993) based on faunal analyses compiled from several industry boreholes on the WCMI have been widely employed by subsequent studies. These estimates are, however, unsuitable in the deep waters of the Laxmi Basin, where drilling data from the IODP sites shows water depths of sedimentation well below shelf values since the end of volcanism. The drilled sequences comprise siliciclastic turbidites dating from ~15 Ma comparable to modern depositional depths. The older Paleocene sediments overlying the basalt are red shales that are also typical deep-water facies. Previous studies suggest that the past sea level fluctuations during early Miocene time submerged large areas of the marginal basin and terminated ongoing delta progradation (Clift, 2006). Palaeo-bathymetry estimates (Mohan, 1985; Raju *et al.* 1999) indicate that the early sedimentation along the WCMI initiated at shallow water depths. Mohan (1985) and Whiting *et al.* (1994) inferred considerable palaeo-bathymetry of the shelf during early Paleocene through late middle Miocene times. Regional palaeo-facies maps (Nair *et al.* 1992;

Zutshi *et al.* 1993) suggest that the major part of the shelf was underlain by marine strata directly over the basaltic basement. Sediments were deposited in deltaic to restricted marine to shallow marine environments (Basu *et al.* 1982; Zutshi *et al.* 1993). Accordingly, we incorporated available palaeo-bathymetric constraints along with the eustatic curves of Haq *et al.* (1987) in our modelling.

## 5. Results and discussion

The stretching factor ( $\beta$ ) is a key parameter that needs to be accounted for when restoring an interpreted section by inverse post-rift modelling. Different  $\beta$  factors cause different rates of post-rift thermal subsidence so that flexural backstripping may allow us to estimate bounds for predicting palaeo-bathymetry or vice versa in an iterative fashion (Kusznir *et al.* 1995; Roberts *et al.* 1998). This is potentially significant because rifting/extension along continental margins cannot be assumed to be laterally uniform. Precise water depth constraints are essential for 1-D backstripping modelling. Since we did not have these constraints across the Laxmi Basin, we believe that 1-D modelling may not provide the best perspective while estimating regional subsidence. Moreover, our seismic profiles are large spaced 2-D regional lines instead of 3-D coverage, so 3-D subsidence analysis would be untenable and unreasonable. Therefore, considering our limitations, we attempted 2-D modelling as the best way to estimate regional flexural subsidence in the present case. The 2-D modelling approach employed here has the flexibility to choose a uniform as well as a laterally varying  $\beta$  profile to determine the best-fit restored cross-section. In order to explore model sensitivity we performed restoration for uniform as well as laterally varying  $\beta$  profiles. By using variable  $\beta$  across the seismic profile, flexural modelling renders more realistic estimates.

The  $\beta$  factor controls the lithospheric flexural strength defined as the effective elastic thickness ( $T_e$ ) (Karner & Watts, 1982). Different  $T_e$  values can render different magnitudes and geometries of deflection, such that low  $T_e$  values generate a large amount of flexure over short distances and high ( $T_e$ ) values result in a small flexural response over greater distances. Sensitivity of reverse, post-rift modelling to lithospheric flexural rigidity was evaluated through a range of plausible  $T_e$  values ( $T_e = 0, 5, 15$  and  $25$  km) and the sediment unloaded basement depths were estimated (for thermo-tectonic as well as thermal subsidence only). A  $T_e$  value of zero would correspond to local isostasy. The modelling results show that the sediment unloaded basement depths are less sensitive when  $T_e$  values are close to zero (Fig. 5). It is also worthy to

note that rifted margins (especially in the presence of large volcanic seamounts as in this case) have low flexural rigidity for several million years after the end of active extension (Karner & Watts, 1982; White, 1999).

In view of the above, we estimated the  $T_e$  at the end of extension by examining the width of the flexural moat around the Raman Seamount. The distance between the centre of the seamount (i.e. the load) and the edge of the flexural trough is  $\sim 55$  km. Assuming a simple flexural relationship and an unbroken plate, this provides an estimate of  $T_e$  of  $\sim 6$  km at the start of Paleocene time. In view of this, a  $T_e$  of 6 km was chosen for reverse post-rift modelling, which is consistent with flexural values for passive margins based on estimates derived from active rifts (White, 1999) as well as forward modelling of sedimentary basins, such as the North Sea and Jeanne d'Arc Basin of Newfoundland (Kuszniir *et al.* 1995). The flexural backstripping analysis was carried out along dip lines IODP-04, W-05 and W-06 and strike lines IODP-01 and IODP-02. The dip lines provide better regional estimates over strike lines because of their greater length and the fact that they cut across the basin structure.

Reverse subsidence modelling of the sedimentary sequences could in theory be used to derive the extension factor in the centre of the basin, but drilling has revealed that the sediments at two IODP sites U1456 and U1457 were deposited in significant water depths. Except for constraining the depth to being above the carbonate compensation depth (CCD) and below the shelf edge ( $>200$  m), no reliable estimates have been derived from these materials (Pandey *et al.* 2016). This means that we have to use other constraints to estimate the extension factor in order to correct for the thermal subsidence. We do this by unloading the sedimentary cover and seamounts from the interpreted sections down to the igneous basement formed by extension during opening of the Laxmi Basin. We then apply a uniform extension model from McKenzie (1978) and, assuming an age of 66 Ma for the end of extension, we then use this unloaded depth to estimate total crustal extension. These values can then be applied in restoring the interpreted section to its estimated water depth since the end of active extension.

### 5.a. Reverse post-rift modelling of IODP-04

The E–W-oriented line IODP-04 (Figs 1, 4) is a  $\sim 450$  km long dip profile orthogonal to the coast and is divided into two domains: the Laxmi Basin (0–340 km from the west) and the shelf margin basin (340–450 km). The boundary between the shelf margin and the deep basin is marked by steeply changing water depths (from 1.8 km to 3.6 km from east to west, respectively). This seismic profile also traverses through short magnetic lineations (Fig. 4) identified in the Laxmi Basin (Bhattacharya *et al.* 1994; Bhattacharya & Yatheesh, 2015). IODP Site U1457 is located on this seismic profile ( $\sim 80$  km from the west end). Drilling and coring at Site U1457 penetrated a total depth of  $\sim 1109$  m below seafloor (mbsf). The thickness of the Cenozoic cover on top of the igneous basement at this site was determined to be  $\sim 1090$  mbsf (Fig. 6).

As an initial exercise, we removed the entire sedimentary and seamount load from across this seismic profile in order to determine the modern depth to basement without the loading effects and with no correction for thermal subsidence. In doing this we were able to generate an estimate of the extension  $\beta$  factors based on the present unloaded depth and an assumed end-rift age of 66 Ma (Figs 7, 8). We used these  $\beta$  factors to estimate the amounts of thermal subsidence through time since the end of extension and

used these values in our reconstructions to progressively correct for this process and separate this from the sediment and water loading effects. Extension appears to have reached a  $\beta$  factor of just under 3 across much of the basin, although this increases to more than 7 in the centre, essentially under the base of the Panikkar Seamount (Fig. 8). A  $\beta$  factor of 7 is very close to full seafloor spreading and might explain the magnetic anomalies in the basin, as melting would be expected (McKenzie & Bickle, 1988). Alternatively, it is possible that seafloor spreading occurred in the basin centre but with more melting than usual and a thicker than normal crust, albeit not on the scale of that seen in classic rifted volcanic margins in the North Atlantic (Planke & Eldholm, 1994) or even other parts of the Arabian Sea (Gaedicke *et al.* 2002; Calvès *et al.* 2011). While extension above a  $\beta$  factor of 3 is typically believed to result in melting and magmatism in the presence of ambient upper mantle (McKenzie & Bickle, 1988; White, 1999), the very high levels of extension in the central part of the basin are consistent with the higher degrees of melting evident by the presence of seamounts (Figs 7, 8). These observations may preclude the basin-wide presence of normal oceanic crust, but do point to very high degrees of extension in the central part of the Laxmi Basin.

The topmost sedimentary unit on this seismic profile corresponds to Pliocene–Recent sediments characterized by strongly reflective sequences with occasional internal onlapping (Fig. 4). Abundant channel-levee complexes are visible in the uppermost part. Based on available stratigraphic knowledge (Kolla & Coumes, 1987; Clift *et al.* 2002; Calvès *et al.* 2008, 2015; Corfield *et al.* 2010; Misra *et al.* 2015) as well as new drilling results from IODP Site U1457, this unit was interpreted as siliciclastic turbidites supplied from the Indus Delta, with intermittent pelagic carbonates (Pandey *et al.* 2016). The underlying upper Miocene–Pliocene is interpreted as submarine fan lobe complexes, as recognized on this profile through their distinct linear strongly reflective characters.

An acoustically transparent layer that thins from north to south and from east to west across the Laxmi Basin (Fig. 4) is observed on this profile. This sequence is interpreted as part of an extensive mass-transport deposit (MTD) known as the Nataraja Submarine Slide (Calvès *et al.* 2015). The MTD is proposed to have been sourced from the Indian shelf edge around the middle–late Miocene boundary before 10.8 Ma (Pandey *et al.* 2016). Pre-dating the MTD is a thin, weakly bedded unit dated as Paleocene based on biostratigraphic markers (Pandey *et al.* 2016). This basal unit overlies rugged basement topography at Site U1457. Under the shelf, this unit is symmetrical to those belonging to the rift onset and break-up unconformities (Pandey *et al.* 2017). The Paleocene unit pre-dates Indus Fan sediments at Site U1457 and pre-dates the onset of India/Eurasia collision (Clift, 2006; Pandey *et al.* 2016).

Reverse post-rift modelling was performed along this profile to reconstruct subsidence since the end of extension ( $\sim 66$  Ma). Earlier extension (India–Madagascar break-up) at 130–120 Ma may have affected the WCMI, but the degree of extension is expected to be low in the Laxmi Basin area (Agrawal & Rogers, 1992; Pandey *et al.* 2017; Mishra *et al.* 2018) so that any residual thermal subsidence had largely decayed by the time of the Laxmi Basin opening. A series of restored cross-sections from the present day to  $\sim 66$  Ma for line IODP-04 is shown in Figure 8. We note that the water depths in the Laxmi Basin are deep through Cenozoic time, consistent with the drilling data, but that the top of the Raman Seamount is close to sea level at the time of its emplacement. This may explain its dimensions and flattish top that may represent a wave-cut platform.

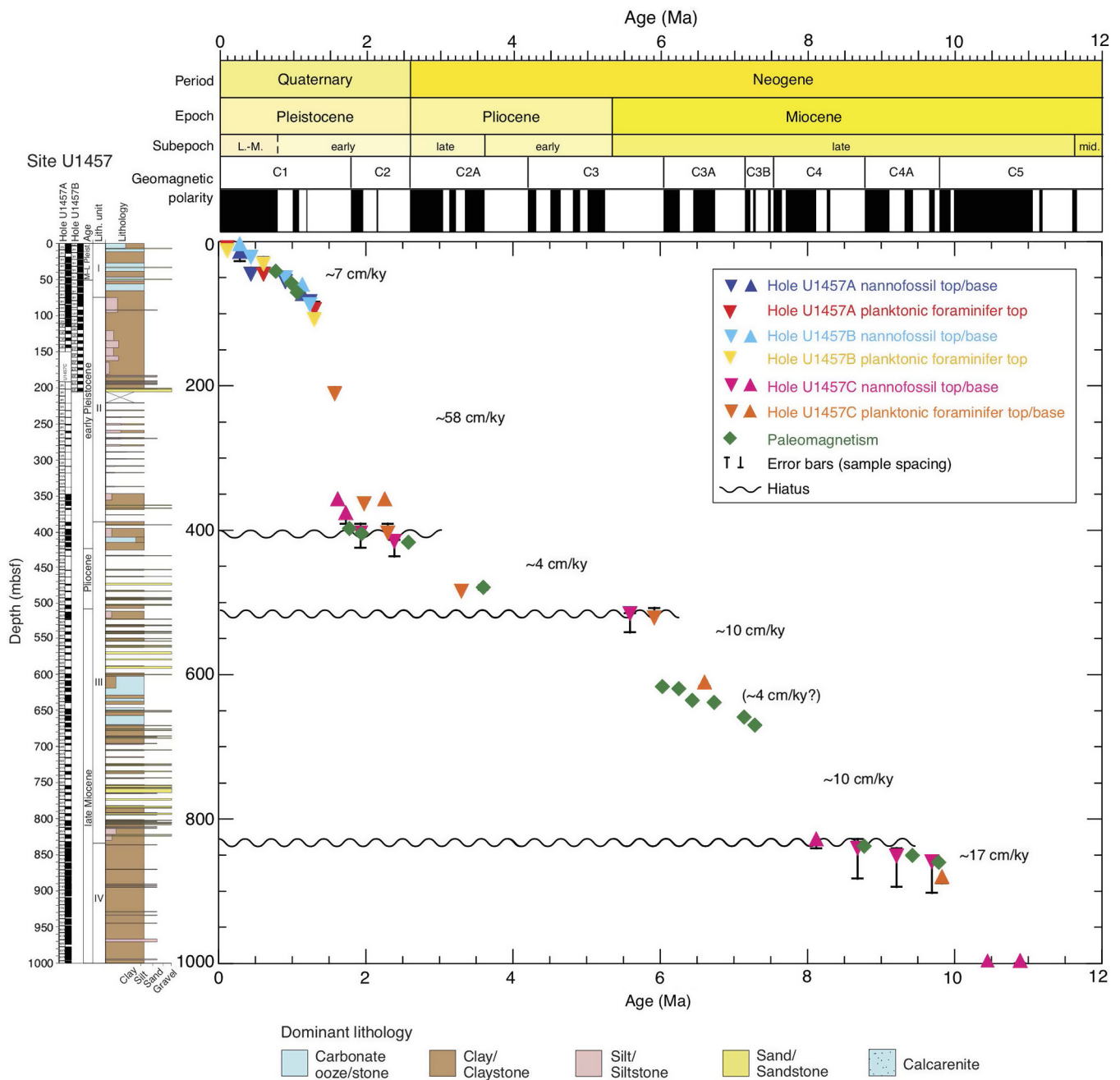


**Fig. 6.** (a) The age-depth model estimated at IODP Site U1457 (after Pandey *et al.* 2016). Numbers (e.g. 10 cm/ky) on the image denote the estimated sedimentation rates for various identified lithological units (on left) based on biostratigraphic/palaeomagnetic markers. An underlying ~30 m thick Paleocene unit and a major mass-wasting deposit emplaced prior to 10.8 Ma are not displayed on this diagram.

If the WCMI had experienced similar high degrees of extension as seen in the Laxmi Basin, then the reverse modelling would have predicted an erosional condition on the shelf in Palaeogene time. However, the palaeo-bathymetry estimates from boreholes on the shelf are inconsistent with such predictions (Mohan, 1985; Whiting *et al.* 1994). Spatial variations in upper crustal structure and a variable  $\beta$  profile better explain the basement topography. Our preferred sequence of restorations with our favoured parameters (Fig. 8) restores elevated parts of the profile closer to sea level compared to the deep Laxmi Basin. A laterally varying  $\beta$  factor from the hyper-extended part of the profile in the west to the shelf

edge in the east is compatible with observations from similar passive margins (Kusznir *et al.* 1995; Roberts *et al.* 1998).

**5.b. Reverse post-rift modelling of strike line IODP-01**

Profile IODP-01 is a ~450 km long NW–SE-oriented strike line in the Laxmi Basin orthogonal to profiles IODP-04 and W-06. The time-depth converted section along this profile (Fig. 9) reveals the present-day stratigraphic succession in the Laxmi Basin. Similar to seismic profile IODP-04, four different stratigraphic units are identified, corresponding to the upper Paleocene to

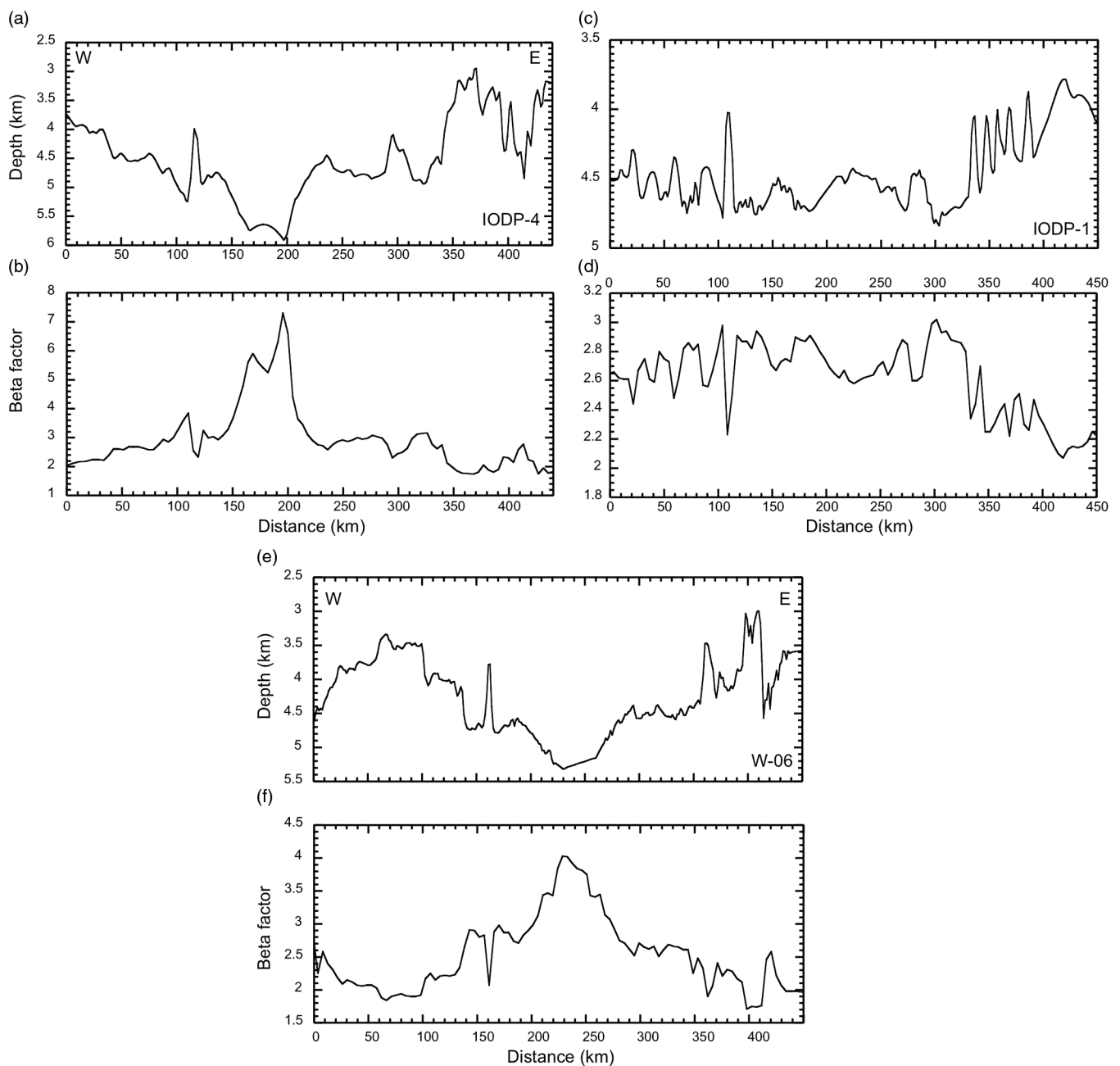


**Fig. 7.** Profiles showing the modern sediment unloaded depth to basement along three different seismic cross-sections in the Laxmi Basin (IODP-04, W-06 profiles and IODP-01) with corresponding estimates of the  $\beta$  factor derived from the uniform extension model of McKenzie (1978).

Recent sediments. Our interpretation is consistent with the drilling and coring at Site U1457 (Pandey *et al.* 2016). The modern water depth along this profile remains largely uniform at ~3.5 km. The sediment unloaded depth to the igneous basement varies around ~4–5 km with intermittent high relief (Fig. 7). The Cenozoic sediment cover thickens at the NW end of the profile, reaching up to >3 km thick. The igneous basement shallows towards the SE end of the profile owing to its proximity to a seamount. Details about identified stratigraphic horizons are provided in Table 1. The back-stripped post-rift restoration to the top of the basement along this profile is shown in Figure 9, using the  $\beta$  factors derived from the unloaded section. The relatively flat bathymetry predicted at the end of extension and the modest changes in extension ( $\beta = 2.2$

to 2.8) means that the slope in the modern basement is largely a function of sediment loading.

### 5.c. Reverse post-rift modelling of strike line W-06

Profile W-06 extends for 450 km across the Laxmi Basin (Fig. 1), within modern water depths of up to 3.5 km and Cenozoic post-rift strata up to 3 km thick (Fig. 10). This profile is located further south than profile IODP-04 discussed in Section 5.a above. IODP Site U1456 is located ~200 km from the western end of the profile (Fig. 10). One of the distinct structural features in the central part of this profile is a subdued volcanic body (~20 km wide, ~2.5 km thick) corresponding to the Panikkar Ridge.



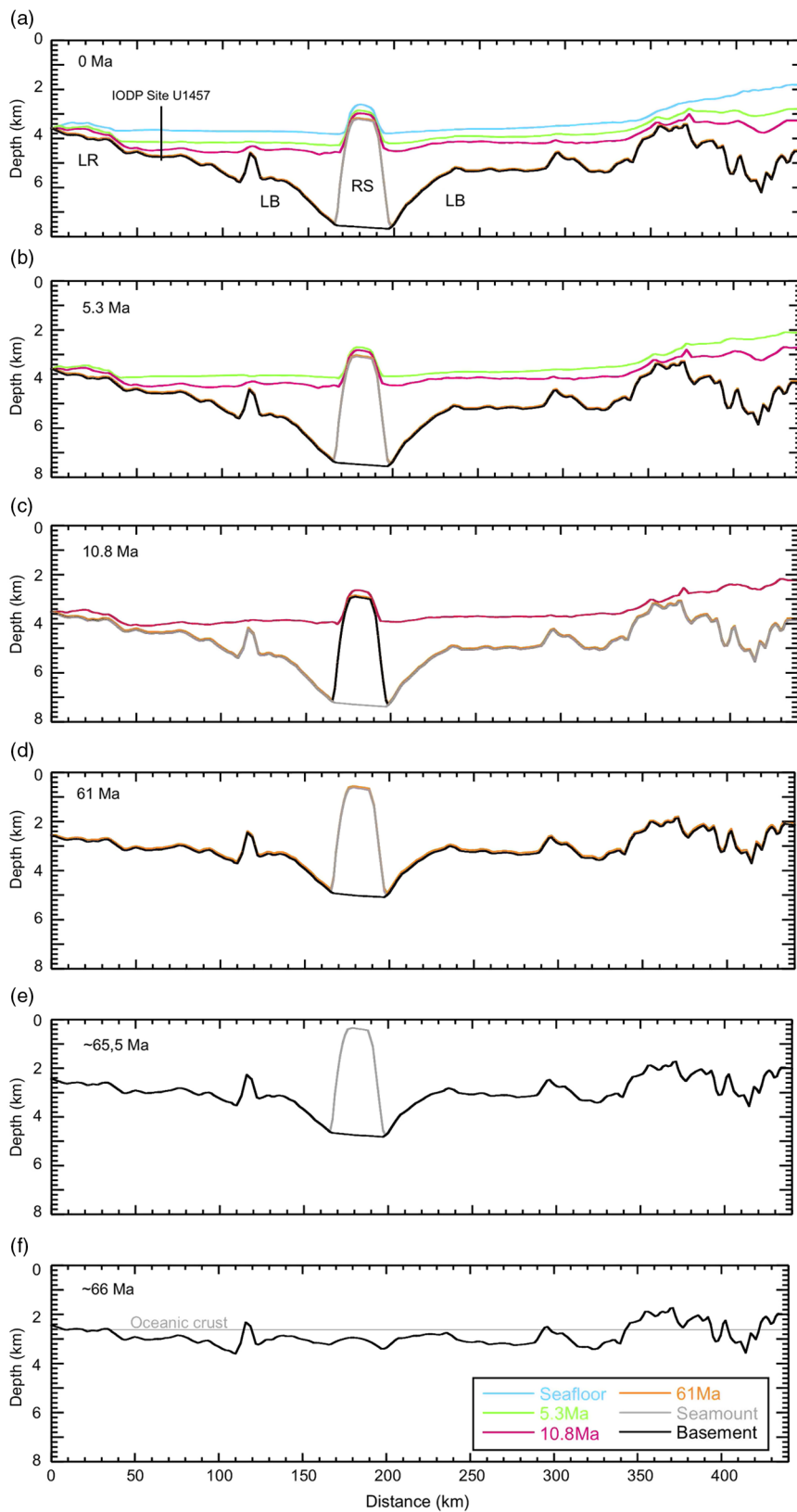


**Fig. 8.** Restored cross-sections for seismic profile IODP-04 at different geological times based on 2-D flexural backstripping analyses. (a) Modern day, and restored stratigraphic sections at (b) 5.3 Ma, (c) 10.8 Ma, (d) 61 Ma, (e) 65.5 Ma after emplacement of the Raman Seamount, and (f) 66 Ma after the end of basin extension. LB – Laxmi basin; LR – Laxmi Ridge; RS – Raman Seamount.

A few late-stage intrusions are also observed on this profile between the Laxmi Ridge and the Panikkar Ridge (Pandey *et al.* 2016; Fig. 9). Detailed stratigraphic interpretation along this profile is discussed by Nair *et al.* (in review). The Cenozoic stratigraphy is dominated by the Miocene, including ~100 m of the Nataraja

Slide MTD, overlain by Pliocene–Recent deposits. Pliocene–Recent successions are characterized by numerous channel-levee feeder systems, as well as onlapping deposits. The western end of the profile crosses the Laxmi Ridge (Fig. 10), which is a sediment-starved basement high structure in this location. Some

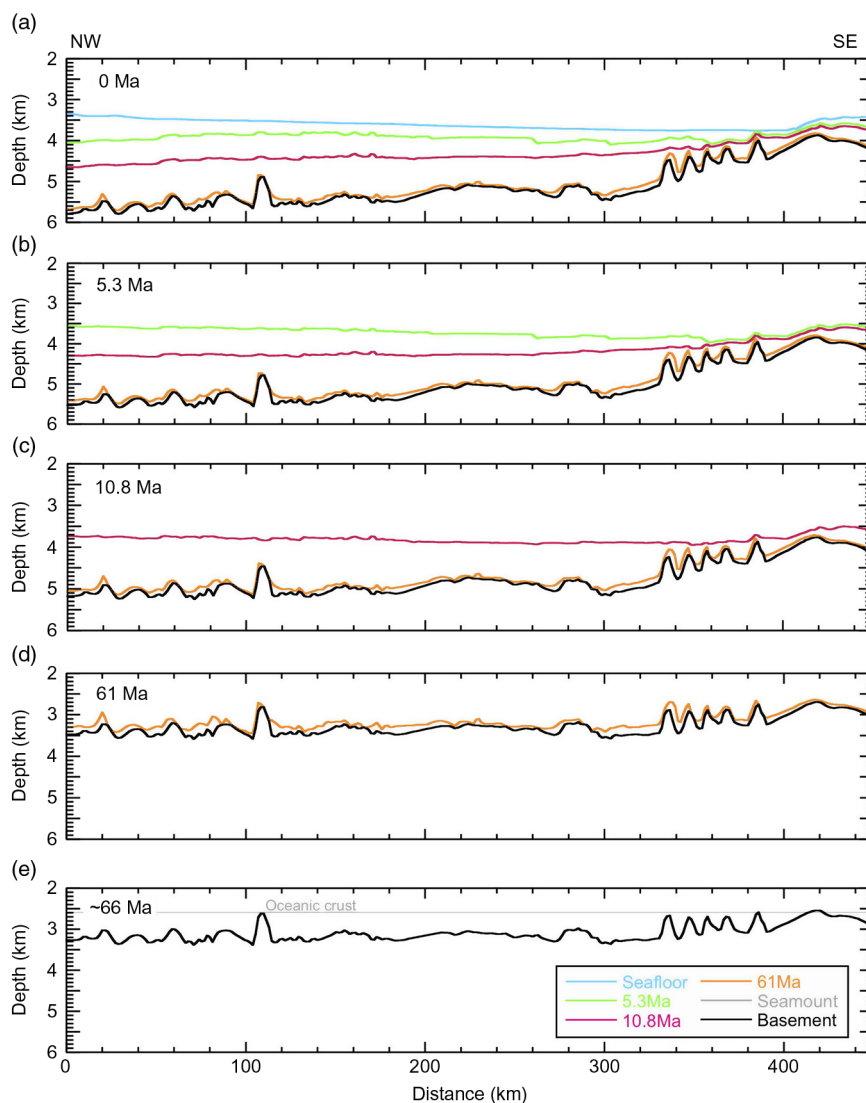


**Fig. 9.** Restored cross-sections along the strike line IODP-01 in the Laxmi Basin at different geological times. (a) Modern day, (b) restored stratigraphic section at 5.3 Ma, (c) 10.8 Ma, (d) 61 Ma, and (e) 66 Ma after the end of basin extension.

signatures of compressional episodes are observed in the surrounding regions, in the form of localized folding in upper Neogene and Paleocene strata (Fig. 10).

The results of backstripping W-06 are shown in Figure 10. The Pliocene–Recent successions have a minimal effect on the palaeo-water depth restorations, largely because they are thin. The greater and varying thickness of the Miocene and older succession has a larger effect on loading, especially of the flexural moat around the Panikkar Ridge (Fig. 10). The restored model along this profile exhibits a reduced residual topography of  $\sim 1.5$  km, suggesting that most of the modern variation is related to loading either by the sediment cover or by the Panikkar Ridge.

It is important to note that the unloaded basement topography on regional seismic profiles in the Laxmi Basin fails to restore close to sea level and exhibits considerable palaeo-bathymetric variations that reflect the variable extension across the basin. Calvès *et al.* (2008) argued that after break-up along the WCMI at 65 Ma, the basement, at least close to the Murray Ridge, experienced only 400 m of thermal subsidence in the 28 Ma before 37 Ma, after which rapid subsidence occurred. These observations have a direct bearing on the rifted margin evolution along the WCMI. Typically, mantle plumes and their related uplift and subsidence might be predicted to cause anomalous subsidence at rift margins (Sleep,

1990; Clift, 2005). Our restoration of the Raman Seamount close to sea level at the end of its eruption, based on correcting for simple thermal subsidence, suggests that if the region had experienced any transient uplift then this must have been rather modest, less than the 340 m predicted palaeo-bathymetry at the top of the seamount. Earlier studies of subsidence anomalies related to the Deccan Flood Basalt/Réunion Hotspot argue for this not being a major cause of uplift (Calvès *et al.* 2008) and our work is consistent with this. The precise timing, extent and locations of rifting in the Arabian Sea prior to  $\sim 61$  Ma are debated (Pandey *et al.* 2016).

Based on our modelling results, we further evaluate if any oceanic crust was created within the Laxmi Basin at or before  $\sim 66$  Ma. Assuming typical thermal subsidence for a normal oceanic crust, Stein & Stein (1992) predicted an average depth of 5.25 km at 66 Ma. This assumption, however, does not account for involvement of any other tectonic process during the new crust formation. Almost all the crust in the Laxmi Basin restores to modern sediment unloaded depths of less than this value, implying that widespread seafloor spreading either did not occur or was limited to the central parts of the basin. Thus, one would expect to find strongly extended continental crust under the Laxmi Basin, assuming that the initial crust was of normal thickness. Thicker than normal oceanic crust would also produce shallower than normal depths, but

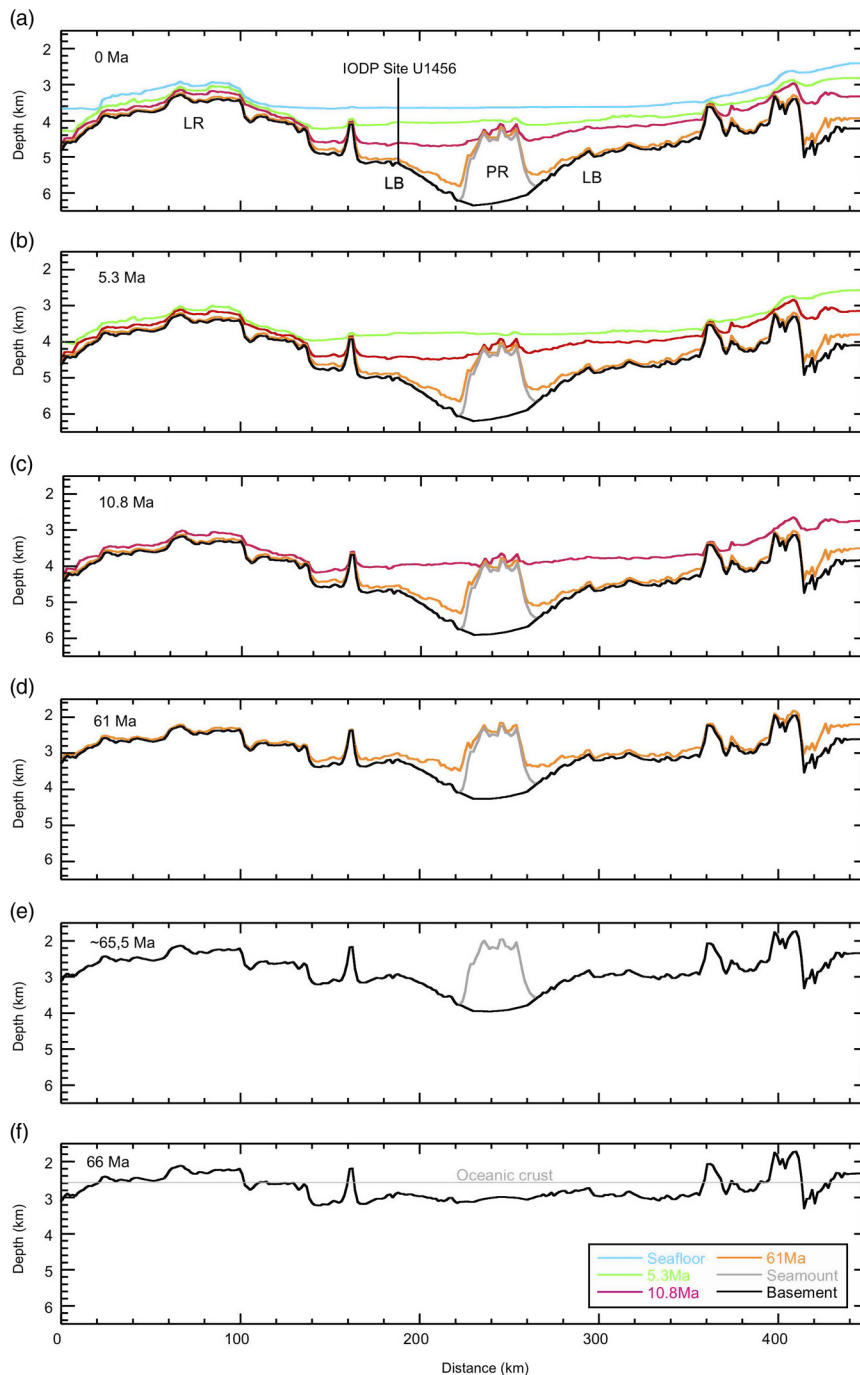


**Fig. 10.** Restored cross-section along dip profile W-06 through its development. (a) Modern day, and restored stratigraphic sections at (b) 5.33 Ma, (c) 10.9 Ma, (d) 61 Ma, (e) immediately after eruption of the Panikkar Ridge, and (f) after the end of extension at 66 Ma. PR – Panikkar Ridge; LR – Laxmi Ridge; LB – Laxmi Basin.

there is no evidence for anomalous high degrees of magmatism, such as depth anomalies that would be predicted to be associated with a mantle thermal anomaly (Sleep, 1990), let alone the large anomalies linked to plume initiation (Farnetani & Richards, 1995).

Research from mid ocean ridges suggests that zero-age oceanic crust lies in ~2–3 km (2.6 km mean) of water and is in equilibrium with a ‘standard’ continental lithospheric column. Using the equation for the initial syn-rift subsidence (Allen & Allen, 2006), the stretching factor required to produce ~2.5 km of subsidence would be >3, as shown by our estimates in Figure 7. This in turn would reduce the total crust to ~9–10 km thick, which would most likely be highly fractured. Under such a scenario, wherever such depths

would be reached, asthenospheric upwelling and rupture are highly likely. White & McKenzie (1989) and, subsequently, Roberts *et al.* (1998) showed that while rifting, a sufficiently large  $\beta$  factor (e.g. >3) can lead to substantial addition of melt at the base of the crust. Although, dispersal of an asthenospheric temperature anomaly may lead to >2 km of additional subsidence (Clift *et al.* 1995), the thickening of the crust through magmatic underplating would lead to a reduction in the total amount of subsidence. Thus, based solely on the subsidence data, we cannot rule out seafloor spreading in the Laxmi Basin but we favour a model of hyper-extension and associated magmatism, especially as initial trace-element discrimination plots indicate that the basement basalts at Site U1457

have an arc-type signature that would imply some extent of lithospheric recycling in addition to melting from the asthenosphere (Pandey *et al.* 2016). The high  $\beta$  factors (Figs 8, 10) and other corroborating information (Pandey & Pandey, 2015; Pandey *et al.* 2017) imply that extremely high stretching/thinning in the Laxmi Basin had occurred prior to ~61 Ma.

Additional evidence for extreme crustal thinning is deduced from the seamounts in the Laxmi Basin that are flanked by deep flexural moats at their bases (Figs 3, 4). Magnetic anomalies from the Laxmi Basin suggest that extension, possibly involving seafloor spreading in the latter stages, was active until ~64 Ma (Chron 28; Bhattacharya *et al.* 1994) or ~56 Ma (Chron 25; Bhattacharya & Yatheesh, 2015). Biostratigraphy from Site U1457 rules out the younger of these two models. If these magnetic interpretations are correct, emplacement of axial seamounts could be younger than Anomaly 28 (~64 Ma) over highly attenuated crust, although the non-hotspot type geochemistry of the basement at Site U1457 would favour eruption before the emplacement of the Deccan Trap volcanic sequences at 66 Ma. Thus, the predicted residual depth anomalies in the Laxmi Basin require explanation through possible tectonic mechanisms (especially prior to ~61 Ma) that could accommodate their large magnitudes. Any possible transient (e.g. plate reorganization) or permanent tectonism (e.g. depth-dependent stretching) that could drive considerable subsidence would also be evident from intra-plate flexure, dynamic support or syn-rift activities, respectively. Short-term tectonic movements typically occur across continental margins (or abyssal basin) in response to the intra-plate stresses (e.g. Cloetingh *et al.* 1990). Such stress distributions are capable of generating flexural deflections across margins, but often their amplitudes are low, up to a few hundred metres, and reversible after the stress relaxation (Cloetingh *et al.* 1990). However, this mechanism by itself is insufficient to account for the observed subsidence in the Laxmi Basin, which we show is compatible with simple thermal subsidence following rifting in latest Cretaceous time. Movements of larger amplitude, up to kilometre scale, could be linked to the dynamic topography above mantle convective flows (e.g. Clift *et al.* 1995; Hopper & Buck, 1996) for which we have no evidence in the Laxmi Basin.

Pandey *et al.* (2017) argued that anomalous subsidence along the WCMI may be related to upper mantle convective circulation associated with rifting in the eastern Arabian Sea. Irreversible subsidence anomalies have also been suggested to result from depth-dependent stretching of lithosphere, which may result in subsidence in excess of that predicted from observable normal faulting where an upper layer (e.g. the upper crust) is stretched to a greater degree than a lower, denser layer (Kusznir *et al.* 2004). Other possible causes for the residual bathymetry could be associated with an earlier phase of rifting (Mesozoic?). However, such possibilities can only be confirmed through study of deeper crustal structure below the present basement from the shelf. In view of the above discussion, we argue that the large subsidence observed in the Laxmi Basin may have resulted from a combination of mechanisms, involving both permanent effects of previous lithospheric extension, as well as to some extent transient responses to its interaction with mantle convective flow. In general, we favour a simple model of hyper-extension in the basin in Late Cretaceous time with limited magmatism and underplating after the end of extension and followed by thermal subsidence, with no significant influence of a major asthenospheric thermal anomaly. However, we also recognize that such propositions are seldom straightforward owing to potential uncertainties and require an in-depth imaging of the crust in the region.

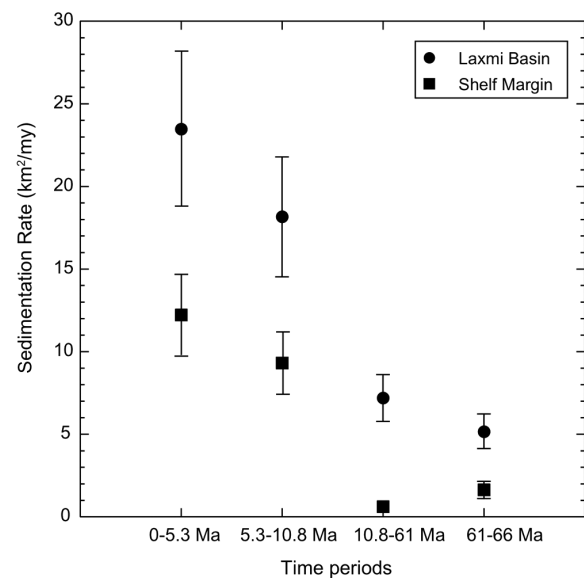


Fig. 11. Computed mass accumulation rates from the decompacted sediment thickness for various periods using pseudo-wells along seismic line IODP-04 in the Laxmi Basin (0–340 km) and shelf margin (340–450 km). See text for details.

#### 5.d. Sediment accumulation rates

The unloaded sediments along each profile provide quantitative estimates of sedimentation rates in the Laxmi Basin since the end of rifting. We estimate sedimentation rates based on the unloaded section IODP-4, described above. Sediment accumulation rates along representative seismic profile IODP-04 are shown in Figure 11, with values calculated based on cross-sectional area if each depositional unit was unloaded and the sediment decompacted to restore it to the original thickness at the end of its deposition following removal of the overlying sequences. The dip profile is divided into two structural domains, namely the Laxmi Basin (0–340 km), which is dominantly filled by supply from the north, mostly the Indus Fan, and the shelf marginal basin (341–450 km), which represents sediments supplied directly from peninsular India. Given the contrasting climate and tectonic conditions of the two sources regions, sediment supply rates might reasonably be expected to be different in these two zones. Rates were estimated for the dated geological periods described in the model. The results show that the fastest sedimentation in the Laxmi Basin and on the continental shelf occurred since 5.3 Ma (Fig. 11) and experienced a major increase after 10.8 Ma.


Sediment accumulation rates were extremely low during Paleocene time, consistent with the drilling results from IODP Site U1457. The Paleocene sedimentation must have been dominantly driven by flux from the Indian passive margin, as well as limited weathering and brecciation of underlying igneous basement, because the Paleocene sequence pre-dates India–Eurasia collision and thus precludes any supply from a palaeo-Indus River. High sedimentation rates during middle Miocene time mostly reflect the emplacement of the Nataraja Slide MTD (Fig. 11). Clift *et al.* (2002), Clift & Gaedicke (2002) and Gupta *et al.* (2004) inferred significantly enhanced sedimentation in the Arabian Sea during the middle–late Miocene period, attributing it to the accelerated mass flux from the Indus River during this time period, including of one of the largest MTDs in this region underlying the upper Miocene (Calvès *et al.* 2015; Pandey *et al.* 2016). Thus, the high sediment accumulation appears to have been sourced from the Indus Fan as well as the observed MTD.

The sediment accumulation rates estimated above are broadly consistent with the biostratigraphically estimated sedimentation rates from Site U1457 (Pandey et al. 2016). Calculated sedimentation rates at Site U1457 (Fig. 6) show that the sedimentation rate during late Miocene time was  $\sim 17 \text{ cm ka}^{-1}$ , which then slowed to  $\sim 10 \text{ cm ka}^{-1}$  before again slowing down to  $\sim 4 \text{ cm ka}^{-1}$  during late Pliocene to early Pleistocene times, albeit interrupted by a phase of very rapid accumulation ( $58 \text{ cm ka}^{-1}$ ) when the drill site lay on a depositional lobe. However, the long-term rates at Site U1457 are  $51 \text{ m Ma}^{-1}$  from 10.8 to 5.3 Ma and then  $95 \text{ m Ma}^{-1}$  after that time. Increasing erosion rates after 5.3 Ma are consistent with models arguing for enhanced continental erosion in the context of the changing climatic cycles after onset of Northern Hemisphere glaciation (Zhang et al. 2001).

## 6. Conclusions

Flexural subsidence modelling of the Laxmi Basin using deep-penetrating seismic reflection profiles provides a basin-wide overview of post-rift subsidence and sedimentation. New seismic data, in association with the scientific drilling at Site U1457, offer new insights into the basement tectonics and cumulative subsidence in the Laxmi Basin since Paleocene time. Based on the restored sections and modelled stretching factors, it is inferred that the Laxmi Basin has undergone extreme stretching of pre-existing crust since Late Cretaceous time. This observation is also consistent with a transitional/oceanic crust in the basin centre.

Rates of subsidence throughout Neogene and Palaeogene times are presumed to have followed normal thermal subsidence patterns in this basin, which restores the top of the Raman Seamount to close to sea level after its eruption. The 340 m discrepancy may reflect inaccurate estimates of the  $\beta$  factor in the basin centre or a moderate loss of dynamic support since that time. There is no evidence for kilometre scale uplift driven by the Deccan plume. Backstripping and decompaction-derived sediment accumulation rates show that maximum sedimentation occurred during Plio-Pleistocene time, similar to many basins worldwide (Zhang et al. 2001). The initial increase dates from 10.8 Ma.

**Author ORCIDs.**  D. K. Pandey 0000-0001-6899-8995, Nisha, Nair 0000-0002-2847-3120, Denise K. Kulhanek 0000-0002-2156-6383

**Acknowledgements.** This research is based on knowledge from analyses of core samples provided by the IODP, and data collected onboard the vessel JOIDES Resolution (IODP Expedition 355–Arabian Sea Monsoon). DP, AP, NN, PR and RR thank the Director, NCPOR for the permission to publish this manuscript. Support for the IHS-Kingdom™ license is gratefully acknowledged. The authors also thank Dr Alan Roberts and Prof. Nick Kusznir for their help with the FLEX-DECOMP™ package. PC's involvement was supported by the Charles T. McCord Chair in Petroleum Geology at LSU. The manuscript benefitted significantly from constructive reviews from the editor as well as anonymous reviewers. This is NCPOR contribution no. 57/2018.

## References

- Agrawal A and Rogers JJW** (1992) Structure and tectonic evolution of the western continental margin of India: evidence from subsidence studies for a 25–20 Ma plate reorganization in the Indian Ocean. In *Basement Tectonics 8: Characterization and Comparison of Ancient and Mesozoic Continental Margins – Proceedings of the 8th International Conference on Basement Tectonics*, pp. 583–90. Dordrecht, The Netherlands: Kluwer Academic Publishers.
- Allen PA and Allen JR** (2006) *Basin Analysis: Principles and Applications*. Oxford: Blackwell Publishing Ltd, 549 pp.
- Basu DN, Banerjee A and Tamhane DM** (1982) Facies distribution and petroleum geology of the Bombay offshore basin, India. *Journal of Petroleum Geology* **5**, 51–75.
- Baxter K, Cooper GT, Hill KC and O'Brien GW** (1999) Late Jurassic subsidence and passive margin evolution in the Vulcan Sub-basin, northwest Australia: constraints from basin modelling. *Basin Research* **11**, 97–111.
- Bhattacharya GC, Chaubey AK, Murty GPS, Srinivas K, Sarma KVLNS, Subrahmanyam V and Krishna KS** (1994) Evidence for seafloor spreading in the Laxmi basin, northeastern Arabian Sea. *Earth and Planetary Science Letters* **125**, 211–20.
- Bhattacharya GC and Yatheesh V** (2015) Plate-tectonic evolution of the deep ocean basins adjoining the western continental margin of India—A proposed model for the early opening scenario. In *Petroleum Geosciences* (ed. S Mukherjee). Cham: Indian Contexts, Springer Geology.
- Biswas SK** (1982) Rift basins in western margin of India and their hydrocarbon prospects with special reference to Kutch Basin. *American Association of Petroleum Geologists Bulletin* **66**, 1497–513.
- Biswas SK** (1989) Hydrocarbon exploration in western offshore basins of India. *Geological Survey of India Special Publication* **24**, 185–94.
- Biswas SK** (1999) A review on the evolution of the rift basins in India during Gondwana with special reference to Western Indian basins and their hydrocarbon prospects. *Proceedings of Indian National Science Academy* **65**, 261–83.
- Calvès G, Clift PD and Inam A** (2008) Anomalous subsidence on the rifted volcanic margin of Pakistan: no influence from Deccan plume. *Earth and Planetary Science Letters* **272**, 231–9.
- Calvès G, Huuse M, Clift PD and Brusset S** (2015) Giant fossil mass wasting off the coast of West India: the Nataraja submarine slide. *Earth and Planetary Science Letters* **432**, 265–72.
- Calvès G, Schwab AM, Huuse M, Clift PD, Gaina C, Jolley D, Tabrez AR and Inam A** (2011) Seismic volcanostratigraphy of the western Indian rifted margin: the pre-Deccan igneous province. *Journal of Geophysical Research: Solid Earth* **116**, doi: 10.1029/2010JB008062.
- Chand S and Subrahmanyam C** (2003) Rifting between India and Madagascar – mechanism and isostasy. *Earth and Planetary Science Letters* **210**, 317–32.
- Chaubey AK, Gopala Rao D, Srinivas K, Ramprasad T, Ramana MV and Subrahmanyam V** (2002) Analyses of multichannel seismic reflection, gravity and magnetic data along a regional profile across the central-western continental margin of India. *Marine Geology* **182**, 303–23.
- Clift PD** (2005) Sedimentary evidence for moderate mantle temperature anomalies associated with hotspot volcanism. In *Plates, Plumes and Paradigms* (eds GR Foulger, JH Natland, DC Presnall and DL Anderson), pp. 279–87. Geological Society of America, Special Paper no. 388.
- Clift PD** (2006). Controls on the erosion of Cenozoic Asia and the flux of clastic sediment to the ocean. *Earth and Planetary Science Letters* **241**, 571–80.
- Clift PD and Gaedicke C** (2002) Accelerated mass flux to the Arabian Sea during the Middle–Late Miocene. *Geology* **30**, 207–10.
- Clift PD, Gaedicke C, Edwards R, Lee JI, Hildebrand P, Amjad S, White RS and Schüller HU** (2002) The stratigraphic evolution of the Indus Fan and the history of sedimentation in the Arabian Sea. *Marine Geophysical Research* **23**, 223–45.
- Clift PD, Turner J and ODP Leg 152 Scientific Party** (1995) Dynamic support of the Icelandic Plume and its effect on the subsidence of the northern Atlantic margins. *Journal of the Geological Society, London* **52**, 935–41.
- Cloetingh S, Gradstein F, Kooi H, Grant AC and Kaminski M** (1990) Plate reorganization: a cause of rapid late Neogene subsidence and sedimentation around the North Atlantic? *Journal of the Geological Society, London* **147**, 495–506.
- Collier JS, Sansom V, Ishizuka O, Taylor RN, Minshull TA and Whitmarsh RB** (2008) Age of Seychelles–India breakup. *Earth and Planetary Science Letters* **272**, 264–77.
- Corfield RI, Carmichael S, Bennett J, Akhter S, Fatimi M and Craig T** (2010) Variability in the crustal structure of the West Indian Continental Margin in the Northern Arabian Sea. *Petroleum Geoscience* **16**, 257–65.
- Courtillot V, Besse J, Vandamme D, Montigny R, Jaeger JJ and Cappetta H** (1986) Deccan flood basalts at the Cretaceous/Tertiary boundary? *Earth and Planetary Science Letters* **80**, 361–74.
- Eagles G and Wibisono AD** (2013) Ridge push, mantle plumes, and the speed of the Indian plate. *Geophysical Journal International* **194**, 670–7.
- Farnetani CG and Richards MA** (1995) Numerical investigations of the mantle plume initiation model for flood basalt events. *Journal of Geophysical Research* **99**, 13813–33.
- Gaedicke C, Schlueter HU, Roeser HA, Prexl A, Schreckenberger B, Meyer H, Reichert C, Clift P and Amjad S** (2002) Origin of the northern Indus Fan

- and Murray Ridge, northern Arabian Sea; interpretation from seismic and magnetic imaging. *Tectonophysics* **355**, 127–43.
- Gaina C, van Hinsbergen DJJ and Spakman W** (2015) Tectonic interactions between India and Arabia since the Jurassic reconstructed from marine geophysics, ophiolite geology, and seismic tomography. *Tectonics* **34**, 875–906.
- Gombos AM, Powell WG and Norton IO** (1995) The tectonic evolution of western India and its impact on hydrocarbon occurrences—an overview. *Sedimentary Geology* **96**, 119–29.
- Gradstein FM, Ogg JG, Schmitz M and Ogg G** (2012) *The Geologic Time Scale 2012*. Amsterdam: Elsevier Publications, 1176 pp.
- Gupta AK, Singh RK, Joseph S and Thomas E** (2004) Indian Ocean high-productivity event (10–8 Ma): linked to global cooling or to the initiation of the Indian monsoons? *Geology* **32**, 753–6.
- Haq BU, Hardenbol J and Vail PR** (1987) Chronology of fluctuating sea levels since the Triassic. *Science* **235**, 1156–67.
- Hopper J and Buck WR** (1996) Effects of lower crustal flow on continental extension and passive margin formation. *Journal of Geophysical Research* **101**, 20175–94.
- Jarvis GT and McKenzie DP** (1980) Sedimentary basin formation with finite extension rates. *Earth and Planetary Science Letters* **48**, 42–52.
- Karner GD and Watts AB** (1982) On isostasy at Atlantic-type continental margins. *Journal of Geophysical Research* **87**, 2923–48.
- Kolla V and Coumes F** (1987) Morphology, internal structure, seismic stratigraphy, and sedimentation of Indus Fan. *American Association of Petroleum Geologists Bulletin* **71**, 650–77.
- Krishna KS, Rao DG and Sar D** (2006) Nature of the crust in the Laxmi Basin (14°–20°N), western continental margin of India. *Tectonics* **25**, doi: [10.1029/2004TC001747](https://doi.org/10.1029/2004TC001747).
- Kuszniir NJ, Hunsdale R and Roberts AM** (2004) Timing of depth-dependent lithosphere stretching on the S. Lofoten rifted margin offshore mid-Norway: pre-breakup or post-breakup? *Basin Research* **16**, 279–96.
- Kuszniir NJ, Roberts AM and Morley C** (1995) Forward and reverse modelling of rift basin formation. In *Hydrocarbon Habitat in Rift Basins* (ed. J Lambiase), pp. 33–56. Geological Society of London, Special Publication no. 80.
- Mathur RB and Nair KR** (1993). Exploration of Bombay offshore basin. In *Proceedings of the 2nd Seminar on Petroleum Basins of India*, Dehradun, India, Vol. 2, pp. 365–96. KDMIPE and ONGC, Indian Petroleum Publishers.
- McKenzie DP** (1978) Some remarks on the development of sedimentary basins. *Earth and Planetary Science Letters* **40**, 25–32.
- McKenzie DP and Bickle M** (1988) The volume and composition of melt generated by extension of the lithosphere. *Journal of Petrology* **29**, 625–79.
- McKenzie DP and Sclater JG** (1971) The evolution of the Indian Ocean since the late Cretaceous. *Geophysical Journal of the Royal Astronomical Society* **24**, 437–528.
- Miles PR, Munschy M and Segoufin J** (1998) Structure and early evolution of the Arabian Sea and East Somali Basin. *Geophysical Journal International* **134**, 876–88.
- Minshull TA, Lane CI, Collier JS and Whitmarsh RB** (2008) The relationship between rifting and magmatism in the northeastern Arabian Sea. *Nature Geoscience* **1**, 463–67.
- Mishra A, Chaubey AK, Sreejith KM and Kumar S** (2018) Crustal underplating and effective elastic plate thickness of the Laxmi Ridge, northern Arabian Sea. *Tectonophysics* **744**, 82–92.
- Misra AA, Sinha N and Mukherjee S** (2015) Repeat ridge jumps and micro-continent separation: insights from NE Arabian Sea. *Marine and Petroleum Geology* **59**, 406–28.
- Mitra P, Zutshi PL, Chourasia RA, Chugh ML, Ananthanarayanan S and Shukla B** (1983) Exploration in western offshore basins. *Petroleum Asia Journal* **VI**, 15–24.
- Mohan M** (1985) Geohistory analysis of Bombay high region. *Marine and Petroleum Geology* **2**, 350–60.
- Mohanty SN, Jain M and Jamkhindikar A** (2013) New insight to hydrocarbon potential of shelf margin basin west of DCS area in Mumbai Offshore Basin, India. In *10th Biennial Conference on Hydrocarbon Exploration and Exposition*, Kochi, India, p. 243.
- Naini BR and Talwani M** (1982) Structural framework and the evolutionary history of the continental margin of Western India. In *Studies in Continental Margin Geology* (eds JS Watkins and CL Drake), pp. 167–91. Tulsa: American Association of Petroleum Geologists vol. 34.
- Nair KM, Singh NK, Ram J, Gavarshetty CP and Muraleekrishnan B** (1992) Stratigraphy and sedimentation of Bombay offshore basin. *Journal of Geological Society of India* **40**, 415–42.
- Pandey DK, Clift PD, Kulhanek DK and the Expedition 355 Scientists** (2016) *Arabian Sea Monsoon*. Proceedings of the International Ocean Discovery Program, vol. 355. College Station, Texas: International Ocean Discovery Program.
- Pandey DK, Nair N, Pandey A and Sriram G** (2017) Basement tectonics and flexural subsidence along western continental margin of India. *Geoscience Frontiers* **8**, 1009–24.
- Pandey A and Pandey DK** (2015) Mechanism of crustal extension in the Laxmi Basin, Arabian Sea. *Geodesy and Geodynamics* **6**, 409–22.
- Planke S and Eldholm O** (1994) Seismic response and construction of seaward dipping wedges of flood basalts: Voring volcanic margin. *Journal of Geophysical Research* **99**, 9263–78.
- Raju DSN, Bhandari A and Ramesh P** (1999) Relative sea-level fluctuations during Cretaceous and Cenozoic in India. *ONGC Bulletin* **36**, 185–202.
- Rao PR and Srivastava DC** (1984) Regional seismic facies analysis of western offshore India. *Bulletin of the Oil and Natural Gas Commission* **21**, 83–96.
- Roberts AM, Kuszniir NJ, Yielding G and Styles P** (1998) 2D flexural back-stripping of extensional basins; the need for a sideways glance. *Petroleum Geoscience* **4**, 327–38.
- Royden L and Keen CE** (1980) Rifting process and thermal evolution of the continental margin of eastern Canada determined from subsidence curves. *Earth and Planetary Science Letters* **51**, 343–61.
- Royer J-Y, Chaubey AK, Dyment J, Bhattacharya GC, Srinivas VY and Ramprasad T** (2002) Paleogene plate tectonic evolution of the Arabian and Eastern Somali basins. In *The Tectonic and Climatic Evolution of the Arabian Sea Region* (eds P Clift, D Kroon, C Gaedicke and J Craig), pp. 7–23. Geological Society of London, Special Publication no. 195.
- Sclater JG and Christie PAF** (1980) Continental stretching: an explanation of the post-Mid-Cretaceous subsidence of the central North Sea Basin. *Journal of Geophysical Research* **85**, 3711–39.
- Sleep NH** (1990) Hotspots and mantle plumes: some phenomenology. *Journal of Geophysical Research* **95**, 6715–36.
- Storey M, Mahoney JJ, Saunders AD, Duncan RA, Kelley SP and Coffin MF** (1995) Timing of hotspot-related volcanism and the breakup of Madagascar and India. *Science* **267**, 852–5.
- Stein CA and Stein S** (1992) A model for the global variation in oceanic depth and heatflow with lithospheric age. *Nature* **359**, 123–9.
- Venkatesan TR, Pande K and Gopalan K** (1993) Did Deccan volcanism pre-date the Cretaceous transition. *Earth and Planetary Science Letters* **119**, 181–90.
- Watts AB** (2001) *Isostasy and Flexure of the Lithosphere*. Cambridge, UK: Cambridge University Press, 472 pp.
- White RS** (1999) The lithosphere under stress. *Philosophical Transactions of the Royal Society of London A: Mathematical, Physical and Engineering Sciences* **357**, 901–15.
- White RS and McKenzie D** (1989) Magmatism at rift zones: the generation of volcanic continental margins and flood basalts. *Journal of Geophysical Research* **94**, 7685–729.
- Whiting BM, Karner GD and Driscoll NW** (1994) Flexural and stratigraphic development of the west Indian continental margin. *Journal of Geophysical Research* **99**, 13791–811.
- Whitmarsh RB** (1974) Some aspects of plate tectonics in the Arabian Sea. In *Initial Reports of the Deep Sea Drilling Project vol. 23* (eds RB Whitmarsh, OE Weser, S Ali, JE Boudreaux, RL Fleisher, D Jipa, RB Kidd, TK Mallik, A Matter, C Nigrini, HN Siddiquie and P Stoffers), pp. 527–35.
- Zhang P, Molnar P and Downs WR** (2001) Increased sedimentation rates and grain sizes 2–4 Myr ago due to the influence of climate change on erosion rates. *Nature* **410**, 891–97.
- Zutshi PL, Sood A, Mohapatra P, Ramani KKV, Dwivedi AK and Srivastava HC** (1993) Lithostratigraphy of Indian petroliferous basins. *Documents-V, Bombay Offshore Basin*, **383**, 117 pp. Dehradun: KDMIPE, ONGC.